Electronic Supplementary Material (ESI) for Journal of Materials Chemistry A.
This journal is © The Royal Society of Chemistry 2024

Supporting Information

Tailoring the interface of lithium metal batteries with in situ formed gel polymer electrolyte

*SiXin Jia,[a] Jinxin Xue,[a] Hong Huo,[a] JianJun Zhou,[*a] Lin Li[*a,b]*

[a] *Beijing Key Laboratory of Energy Conversion and Storage Materials, College of Chemistry, Beijing Normal University, Beijing 100875, China*

[b] *College of Textiles & Clothing, Qingdao University, Qingdao 266071, China*

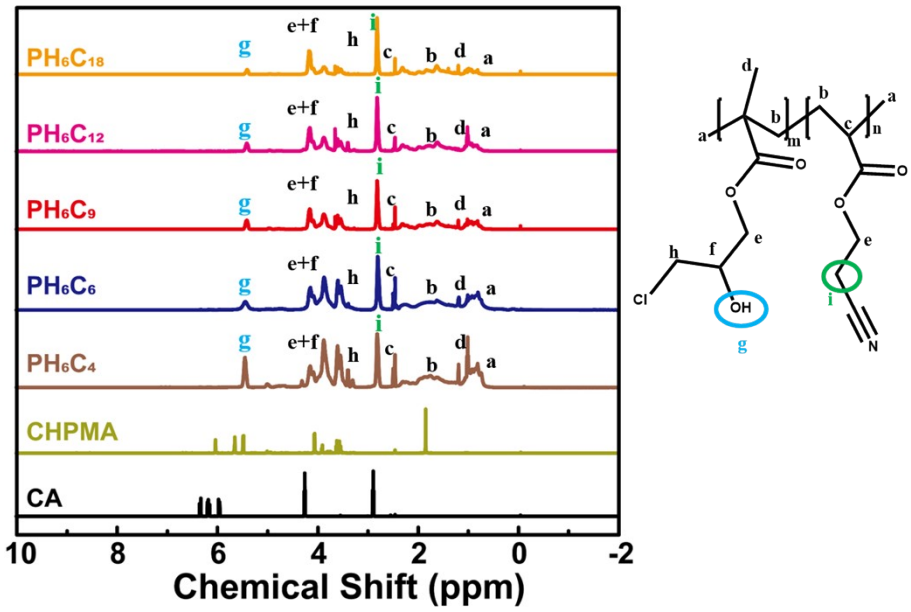

Fig. S1. ^{1}H NMR spectra of monomers and binary copolymers with different proportions.

Table S1. Area ratio of binary copolymer with different feed ratio.

Polymer	Theoretical feed ratio	Theoretical area ratio	Actual area ratio
PH_6C_4	1:0.67	1:1.34	1:1.31
PH_6C_6	1:1.00	1:2.00	1:2.20
PH_6C_9	1:1.50	1:3.00	1:3.18
PH_6C_{12}	1:2.00	1:4.00	1:4.17
PH_6C_{18}	1:3.00	1:6.00	1:6.19

Table S2. The Mn, Mw and polydispersity index (PDI) of PHCs.

PHCs	Mn	Mw	PDI
PH_6C_4	76358	286397	3.75
PH_6C_6	62748	223771	3.57
PH_6C_9	59489	221247	3.72
PH_6C_{12}	65855	217830	3.31
PH_6C_{18}	58597	221321	3.78

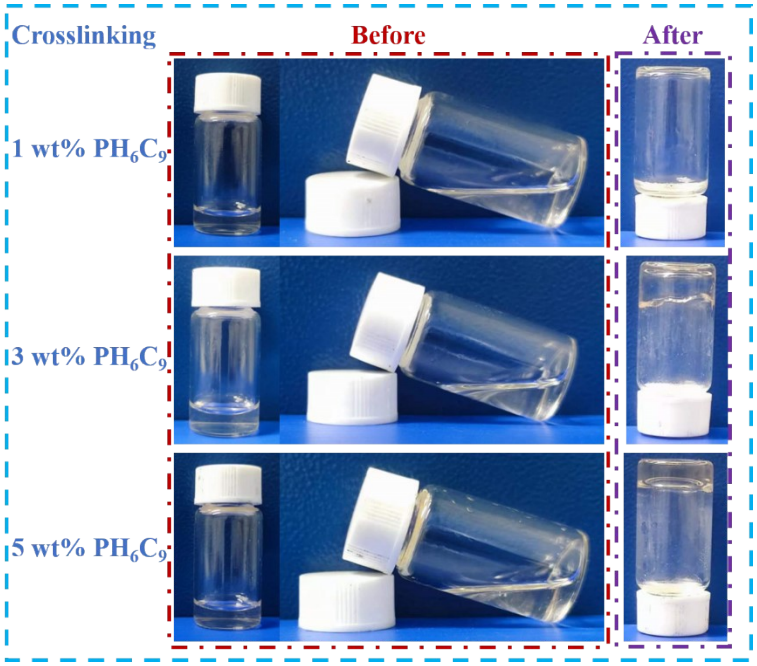

Fig. S2. Photographs of *c*-PH_6C_9-GPE with different content of PH_6C_9.

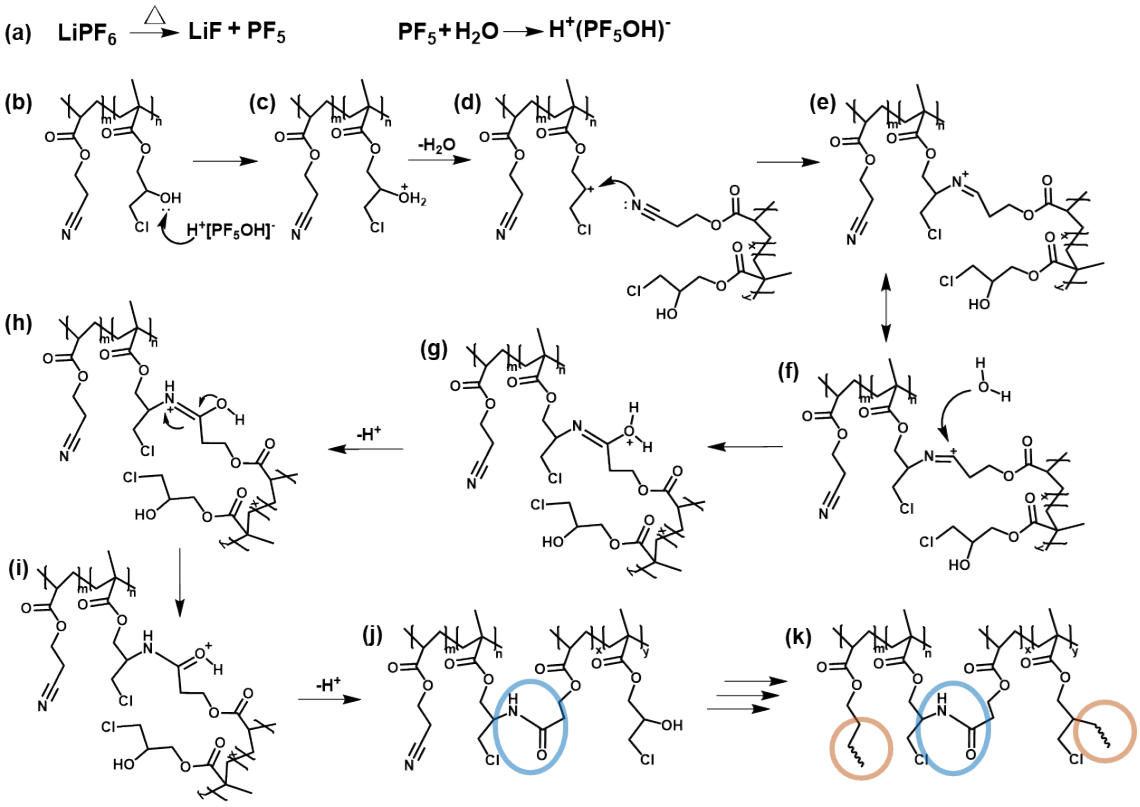

Fig. S3. The cross-linked polymer matrix of *c*-PHC-GPE formed through Ritter reaction.

During heating, a slight number of $LiPF_6$ will decompose to produce LiF and PF_5. PF_5 will combine with trace of H_2O in LE to form $H^+(PF_5OH)^-$, which initiates Ritter reaction (Fig. S3a). The dissociated H^+ will attack the nucleophilic O on hydroxyl group and form H_2O^+ in the side chain (Fig. S3b). The detachment of H_2O lead to the formation of carbocation (Fig. S3c). The electrophilic nitrile group will attack the carbocation ion and form imine cation (Fig. S3d and e). The more stable imine cation capture H_2O, which turns into amide group after tautomerism rearrangement (Fig. S3f-j). The Ritter reaction takes place among chain segments, forming amide covalently cross-linked polymer matrix (Fig. S3k).

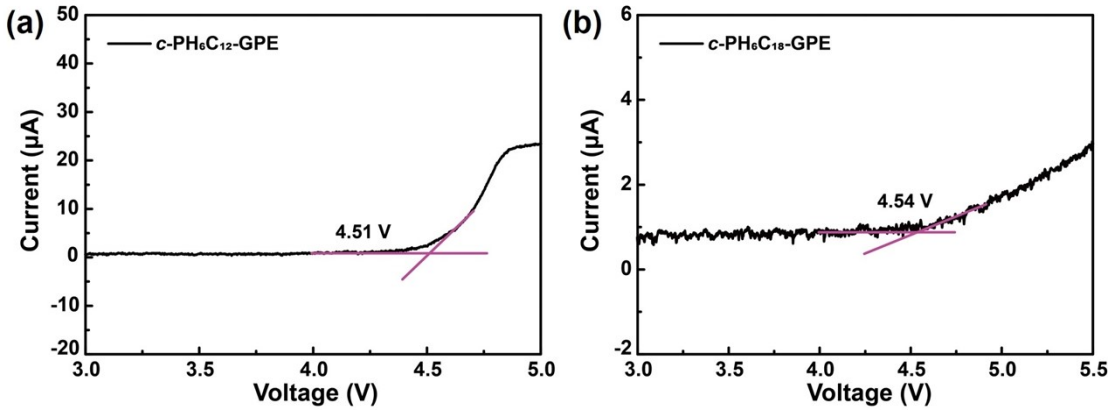

Fig. S4. The LSV curves of *c*-PH_6C_{12}-GPE and *c*-PH_6C_{18}-GPE.

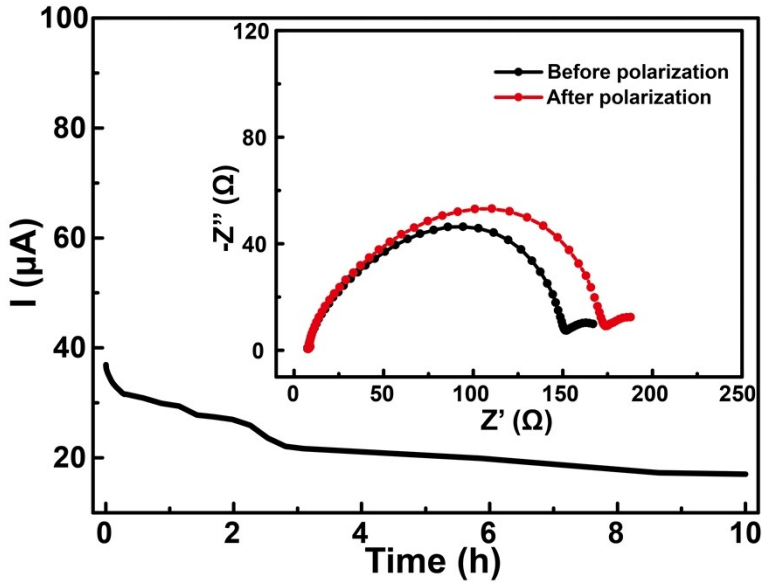

Fig. S5. Polarization curve and impedance curve diagrams of LE.

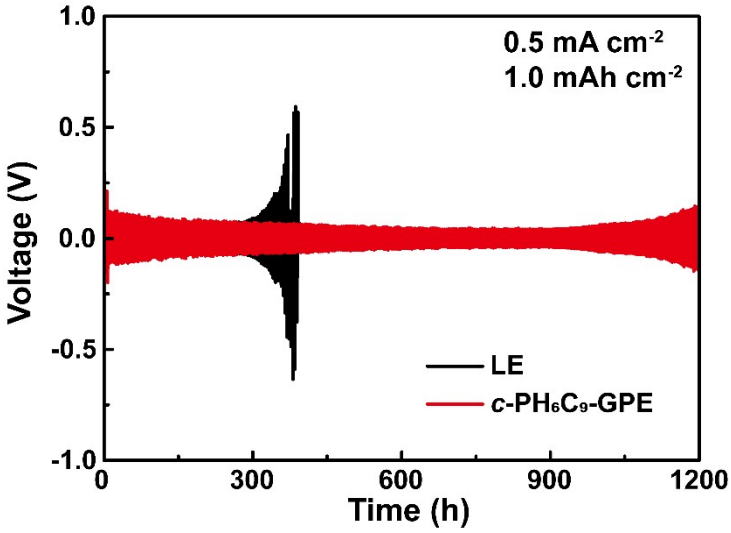

Fig. S6. The potential profiles of Li||Li symmetric batteries with LE and *c*-PH_6C_9-GPEs at a current density of 0.5 mA cm^{-2}.

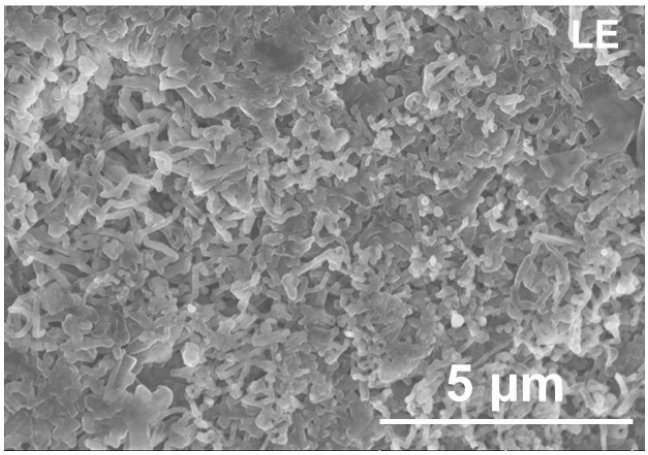

Fig. S7. The surface SEM images of Li anode after cycling with LE.

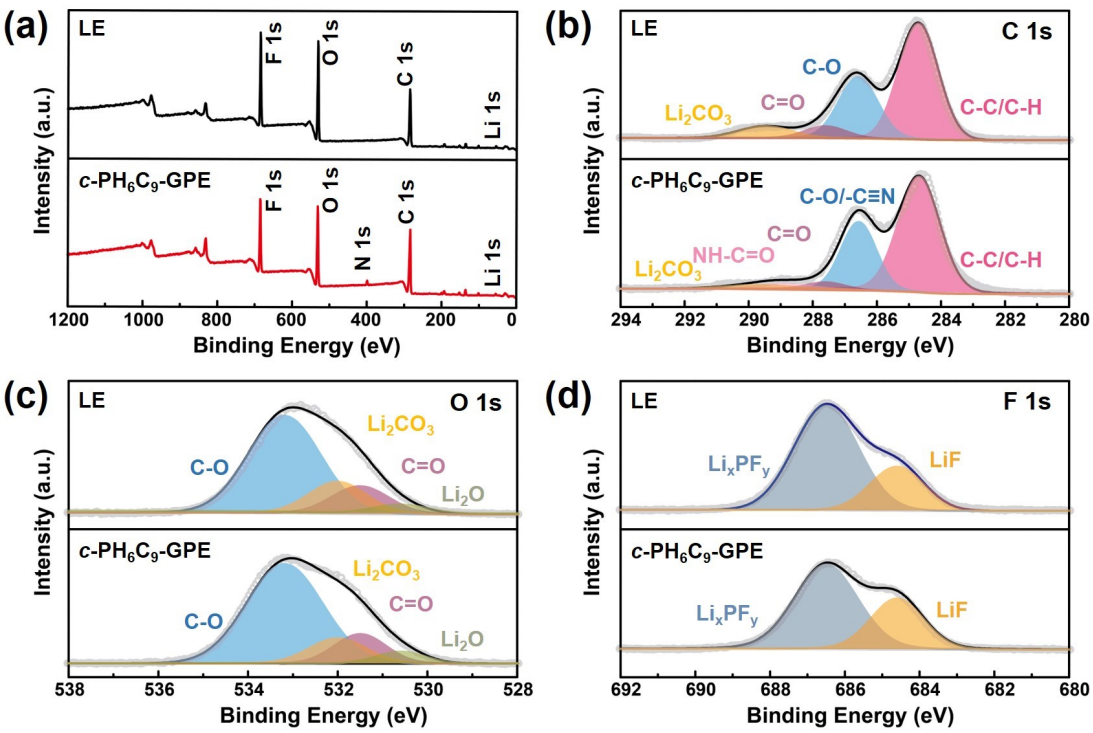

Fig. S8. (a) The survey spectra, (b) C 1s, (c) O 1s and (d) F 1s XPS spectra of Li electrode surface in Li||Li symmetric batteries with LE and *c*-PH_6C_9-GPE.

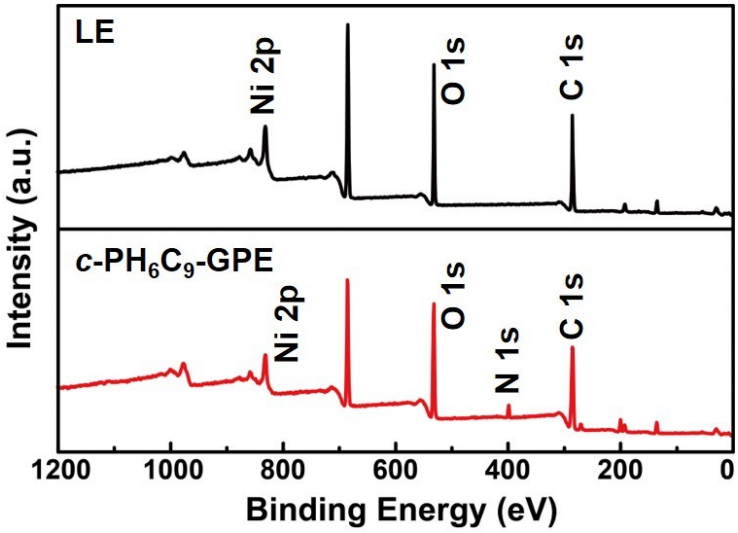

Fig. S9. The XPS survey spectra of NCM622 cathodes from Li|LE|NCM622 and Li|*c*-PH_6C_9-GPE|NCM622 batteries after 50 cycles.

Table S3. The performance comparison of the polymer electrolytes and Li||NCM batteries in the literatures.

Electrolytes	**σ (mS cm^{-1})**	**LSV (V)**	t_{Li^+}	**Cathode**	**Mass loading (mg cm^{-2})**	**Rate (C)**	**Capacity retention ratio (%)**	**Cycle number**	**Ref.**
LiTFSI-LIBF$_4$-Poly(DOL)	1.18	4.8	0.68	NCM811	3.4	1.0	88.6	300	S1
PEGMEMA-SN-LLZT	1.117	5.06	0.627	NCM811	1.5	0.5	61	400	S2
PEO-PVDF/LLZTO	0.361	4.9	/	NCM622	2.5	0.5	77.4	200	S3
MOFLi/MSLi QSE	0.15	0.71	4.6	NCM622	1.0	1.0	70	200	S4
PVFH-PMC-PEGC	2.7	/	0.77	NCM622	1.5	/	93.8	100	S5
GF-SSE-N	1.4	4.5	0.54	NCM622	3.0	0.2	97	50	S6
PAN-PEO-TEGDME	0.038	4.8	0.41	NCM622	1.5	0.1	~60	100	S7
Poly(DOL)	3.03	4.6	0.71	NCM622	4.5	0.5	93	100	S8
P(CUMA-CUEM)-QPE	0.48	5.6	0.47	NCM622	2.0	0.5	78.1	200	S9
***c*-PH$_6$C$_9$-GPE**	**1.20**	**4.89**	**0.68**	**NCM622**	**4.5**	**0.5**	**90.4%**	**200**	**This work**

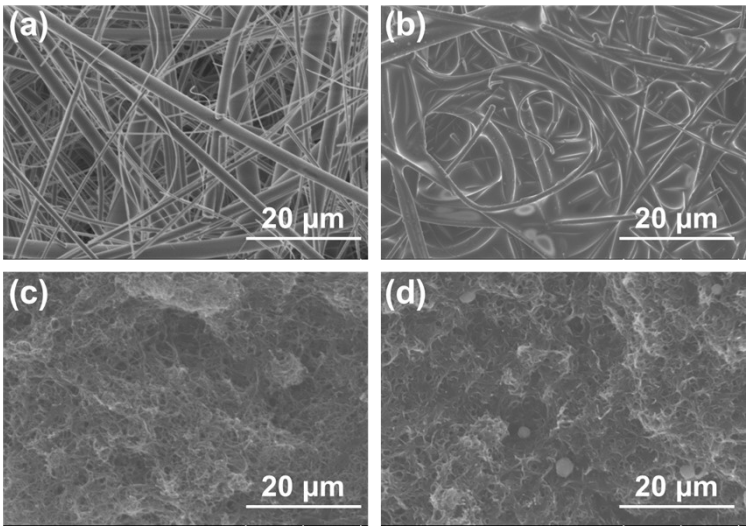

Fig. S10. The SEM images of GF membrane (a) before and (b) after infiltrating and cross-linking. The SEM images of cathode surface (c) before and (d) after infiltrating and cross-linking.

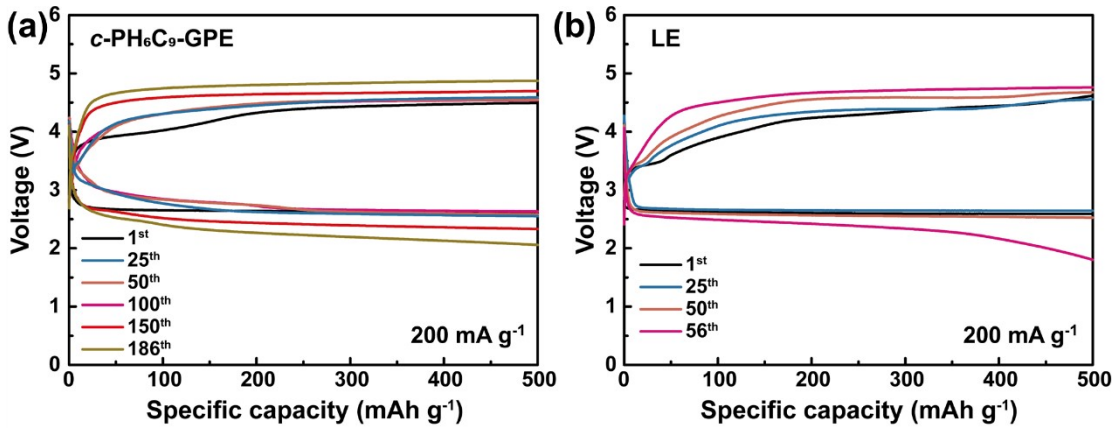

Fig. S11. Discharge/charge curves of Li-O_2 batteries with (a) *c*-PH_6C_9-GPE and (b) LE.

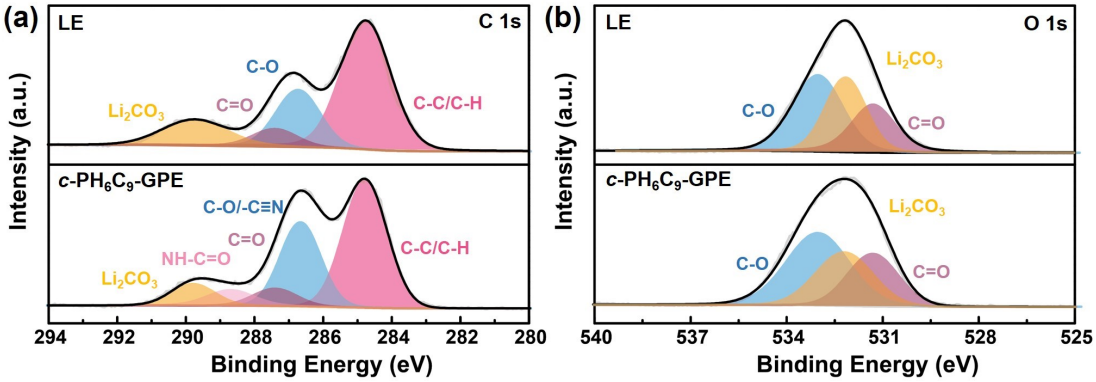

Fig. S12. XPS spectra of cathode surface for Li|LE|O_2 battery and Li|*c*-PH_6C_9-GPE|O_2 battery: (a) C 1s and (b) O 1s.

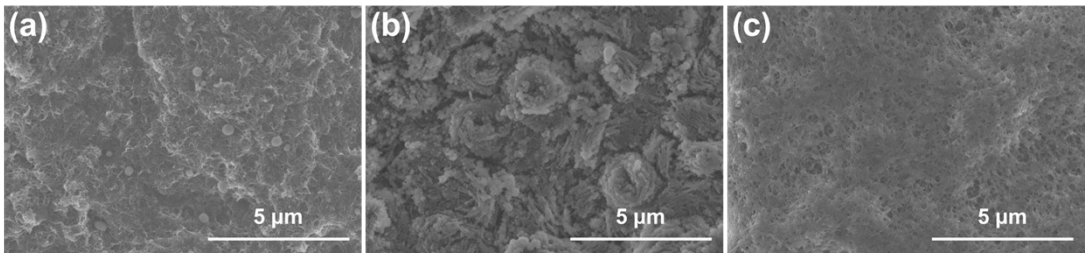

Fig. S13. The SEM images of cathode surface after (a) pristine, (b) the 1st cycle after fully discharged and (c) the 1st cycle after fully charged.

Table S4. The EIS fitted values of the Li-O_2 batteries with LE and *c*-PH_6C_9-GPE.

Battery	Li|LE|O_2		Li|*c*-PH_6C_9-GPE|O_2	
Impedance	R_{SEI} (Ω)	R_{ct} (Ω)	R_{SEI} (Ω)	R_{ct} (Ω)
1st	67.3	64.0	161.5	79.5
20th	78.9	159.1	129.8	64.4
50th	212.1	302.8	82.5	210.5

References

1. Q. Liu, Y. Sun, S. Wang, Q. An, L. Duan, G. Zhao, C. Wang, K. Doyle-Davis, H. Guo and X. Sun, *Mater. Today*, 2023, **64**, 21-30.
2. A. G. Nguyen, M. H. Lee, J. Kim and C. J. Park, *Nano-Micro Lett.*, 2024, **16**, 83.
3. L. Li, Y. Deng, H. Duan, Y. Qian and G. Chen, *J. Energy Chem.*, 2022, **65**, 319-328.
4. Z. Chen, W. Zhao, Q. Liu, Y. Xu, Q. Wang, J. Lin and H. B. Wu, *Nano-Micro Lett.*, 2024, **16**, 114.
5. P. Zhai, W. He, C. Zeng, L. Li and W. Yang, *Chem. Eng. J.*, 2023, **451**, 138414.
6. M. Yang, S. Li, G. Zhang, M. Huang, J. Duan, Y. Cui, B. Yue and H. Liu, *ACS Appl. Mater. Interfaces*, 2023, **15**, 18323-18332.
7. Y. Liu, F. Fu, C. Sun, A. Zhang, H. Teng, L. Sun and H. Xie, *Inorganics*, 2022, **10**, 42.
8. Q. Ma, J. Yue, M. Fan, S. J. Tan, J. Zhang, W. P. Wang, Y. Liu, Y. F. Tian, Q. Xu, Y. X. Yin, Y. You, A. Luo, S. Xin, X. W. Wu and Y. G. Guo, *Angew. Chem. Int. Ed.*, 2021, **60**, 16554-16560.
9. H. Xu, C. Sun, S. Zhang, H. Zhang, Z. Liu, Y. Tang and G. Cui, *ChemSusChem*, 2023, **16**, e202202334.